JACS
JOURNAL OF THE AMERICAN CHEMICAL SOCIETY

Article

Site-Directed Fragment-based Screening for the Discovery of Protein-Protein Interaction Stabilizers

Eline Sijbesma, Kenneth K Hallenbeck, Seppe Leysen, Pim de Vink, Lukasz Skora, Wolfgang Jahnke, Luc Brunsveld, Michelle R. Arkin, and Christian Ottmann

J. Am. Chem. Soc., **Just Accepted Manuscript** • DOI: 10.1021/jacs.8b11658 • Publication Date (Web): 01 Feb 2019

ACS Publications

is published by the American Chemical Society. 1155 Sixteenth Street N.W., Washington, DC 20036

Site-Directed Fragment-based Screening for the Discovery of Protein-Protein Interaction Stabilizers

Eline Sijbesma[†⊥], Kenneth K. Hallenbeck[‡⊥], Seppe Leysen[†], Pim J. de Vink[†], Lukasz Skóra[§], Wolfgang Jahnke[§], Luc Brunsveld[†], Michelle R. Arkin*[,‡], Christian Ottmann*[,†,#]

[†] Laboratory of Chemical Biology, Department of Biomedical Engineering and Institute for Complex Molecular Systems (ICMS), Eindhoven University of Technology, Eindhoven, the Netherlands

[‡] Department of Pharmaceutical Chemistry and Small Molecule Discovery Centre (SMDC), University of California, San Francisco, United States

[§] Chemical Biology and Therapeutics, Novartis Institutes for Biomedical Research, Basel, Switzerland

[#] Department of Chemistry, University of Duisburg-Essen, Essen, Germany

ABSTRACT: Modulation of Protein-Protein Interactions (PPIs) by small molecules has emerged as a valuable approach in drug discovery. Compared to direct inhibition, PPI stabilization is vastly underexplored but has strong advantages, including the ability to gain selectivity by targeting an interface formed only upon association of proteins. Here, we present the application of a site-directed screening technique based on disulfide trapping (tethering) to select for fragments that enhance the affinity between protein partners. We target the phosphorylation-dependent interaction between the hub protein 14-3-3σ and a peptide derived from Estrogen Receptor α (ERα), an important breast cancer target that is negatively regulated by 14-3-3σ. We identify orthosteric stabilizers that increase 14-3-3/ERα affinity up to 40-fold and propose the mechanism of stabilization based on X-ray crystal structures. These fragments already display partial selectivity towards ERα-like motifs over other representative 14-3-3 clients. This first of its kind study illustrates the potential of the tethering approach to overcome the hurdles in systematic PPI stabilizer discovery.

Introduction

Once considered 'undruggable', protein-protein interactions (PPIs) have been successfully targeted by drug-like molecules in the past 15-20 years.[1–4] In contrast to the fruitful development of PPI *disruptors*, examples of targeted small-molecule PPI *stabilizers* are relatively scarce, and dedicated screening approaches for PPI stabilizer identification are virtually absent.[5–7]

Therapeutic proof-of-concept for PPI stabilization has been provided by natural products, including the anti-tumor drug paclitaxel and immune suppressants rapamycin and FK506.[6,7] Additionally, a number of successes using synthetic molecules have been reported, such as the BRD4-dimer stabilizer (biBET)[8] and the allosteric stabilizer of the tetramer transthyretin (tafamidis).[9] Synthetic approaches - proteolysis targeting chimeras (PROTACs) and immunomodulatory drugs (iMiDs) - apply this principle to drive the association of two proteins that would not otherwise interact.[10] These clinical and chemical-biology applications justify the development of technology platforms to allow systematic stabilization of PPI, especially given the fact that most discoveries of PPI stabilizing molecules have been serendipitous. The design rules for a good stabilizer are poorly understood and technical difficulties complicate assay development. There is thus an unmet need for approaches that overcome inherent limitations of conventional ligand screening to identify PPI stabilizers.

We envisioned that disulfide trapping (tethering) would be a promising technology to develop such a platform. Disulfide trapping allows site-directed selection of ligands and readily measures cooperative binding – qualities that address the main challenges posed by screening for PPI stabilizers. Since the technology was pioneered by Wells, Erlanson and co-workers[11], disulfide trapping has successfully identified allele-specific inhibitors of oncogenic KRas (G12C)[12], allosteric ligands of kinase PDK1[13] and inhibitors of the IL-2/IL-2receptor PPI[14,15]. Here, we offer the first demonstration of the tethering technology to identify small-molecule stabilizers of a protein complex.

We selected the interaction between the hub protein 14-3-3 and the phosphorylated motif derived from the breast-cancer-associated transcription factor Estrogen Receptor α (ERα) as a suitable and relevant test case. With >300 cellular interaction partners, including Raf kinases[16], heat shock proteins,[17] oncogenes[18] and tumor suppressors (p53)[19], 14-3-3 proteins are central regulators in many biological processes and pathologies.[20–22] For example, 14-3-3 binding antagonizes multiple transcription factors that act as oncogenic drivers. Since inhibition of transcriptional activity is a central therapeutic challenge in cancer, we have focused our efforts towards identifying small molecule stabilizers for this PPI class. De Vries-van Leeuwen *et al* reported that ERα is phosphorylated at the penultimate residue T594 and that binding of this site to 14-3-3 reduces its estradiol-dependent

transcriptional activity. Inhibition of ERα activity is enhanced by the natural product Fusicoccin A (FC-A), which binds at the 14-3-3/ERα interface (Figure 1a).[18] Stabilizing this PPI was proposed to be a valid alternative strategy for interfering with ERα-positive breast cancer.

Here, we identified several disulfide fragments that each bound cooperatively to a complex of 14-3-3 and ERα-derived phosphopeptide (ERα-pp). Hits selectively increased the binding affinity between ERα-pp and 14-3-3 by as much as 40-fold; multiple x-ray co-structures suggested the mechanism of stabilization. Disulfide tethering is a promising approach to identify starting points to specifically stabilize protein-peptide interactions and provides a first and long-needed, systematic screening platform for PPI-stabilizing molecules.

Results and Discussion

Tethering uses a cysteine on the target protein as a reactivity handle to trap disulfide-containing fragments that have an inherent (weak) binding affinity for a target pocket near the cysteine. The bound fragments can then be detected by intact protein mass spectrometry (MS).[11,23] Our disulfide trapping approach was designed to target FC-A's hydrophobic pocket at the 14-3-3σ/ERα interface. Sigma is the only one of seven human 14-3-3 isoforms that contains a native surface-exposed cysteine (C38) at the edge of this pocket. We further designed two protein constructs in which the wildtype cysteine was mutated (C38N; N being the most common residue at this position) and a cysteine introduced at positions 42 or 45, one or two α-helix turns towards the ERα binding site, respectively (Figure 1a). The three 14-3-3σ cysteine constructs were screened both in *apo* form and in complex with a 15-mer phosphopeptide representing the 14-3-3-binding motif of ERα (ERα-pp; KYYITGEAEGFPA**pT**^{594}V; Figure 1b). Phosphorylated motifs derived from 14-3-3 client proteins recapitulate key interactions of the PPI, and mutating the single phosphorylation site can completely abrogate the interaction *in vitro* and in cells.[24] Short 14-3-3 client-derived phosphopeptides can thus be used *in vitro* as surrogates for the PPI; this approach has been used to characterize FC-A/14-3-3/client complexes and to screen for inhibitors[25], e.g., of the 14-3-3/Tau PPI.[26,27]

Apo-14-3-3σ or the 14-3-3σ/ERα-pp complex was screened against a 1600-member disulfide library under mildly reducing conditions (100 μM betamercaptoethanol; βME). Conjugate formation for each individual reaction was analyzed by intact protein MS. Three peaks observed in mass spectra corresponded to *apo*, βME-capped, and fragment-conjugated 14-3-3σ. The 'percent tethering', defined as the intensity of the fragment-specific conjugate protein peak divided by the sum of the intensities for all protein peaks, was calculated for each individual experiment using an automated pipeline.[28]

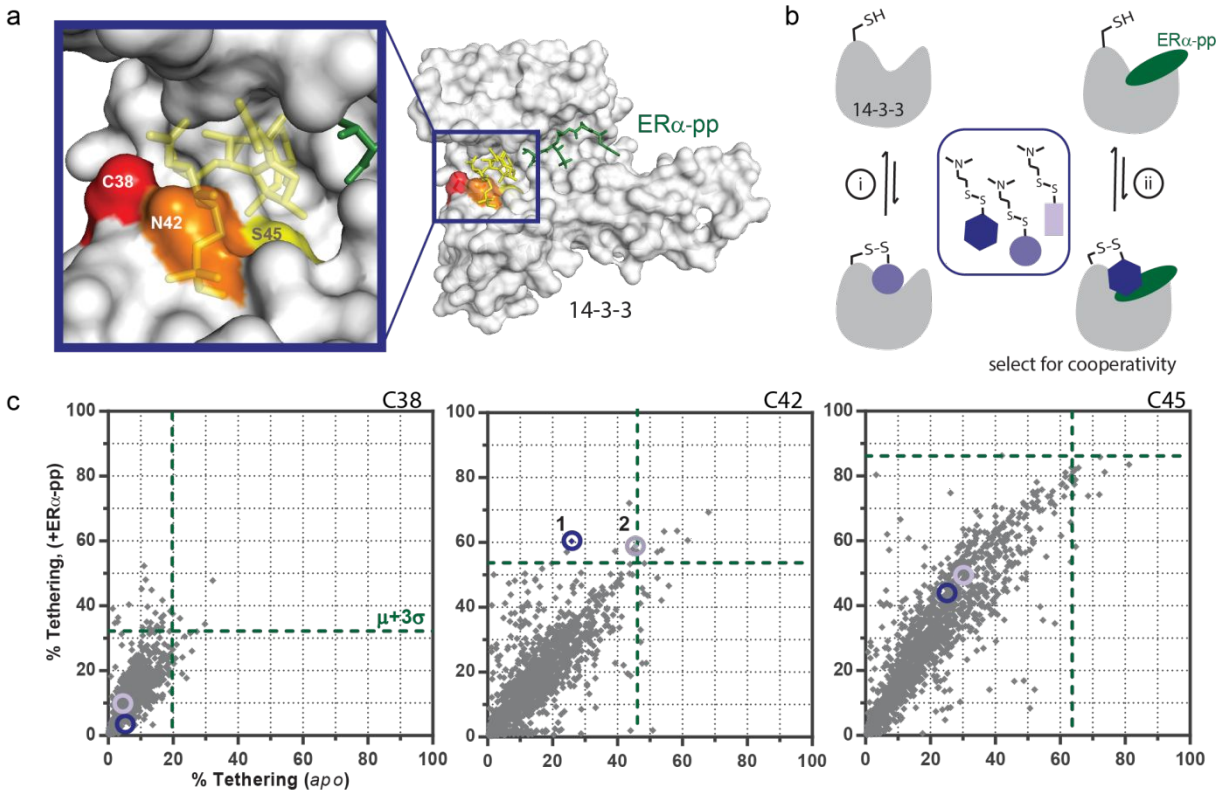

Figure 1. a) The target pocket for stabilizing the interaction of 14-3-3σ (white surface) and ERα-pp (green sticks) bound by FC-A (yellow sticks) (PDB: 4JDD). Indicated are the native cysteine (C38; red surface) and introduced C42 (orange) or C45 (yellow). b) Schematic illustration of the approach for selecting stabilizers by disulfide trapping. The cysteine-containing protein is incubated with an arrayed disulfide-fragment library under reducing conditions in the *apo* state (i) or bound to ERα-pp (ii). The equilibrium is shifted to the fragment-conjugated protein only when it has an inherent affinity for the nearby target pocket. c) 2D-plots illustrate the correlation between % tethering of individual fragments (♦) for *apo* 14-3-3σ and 14-3-3σ/ERα-pp complex. The hit-selection threshold (mean + three standard deviations; μ+3σ) in each screen is indicated by a green dashed line. Fragment **1** (◎) and **2** (◎) are indicated for each screen; both only score as a 'hit' for C42.

For each screen, hits were categorized as competitive (only a hit in the *apo* screen), cooperative (preferentially a hit for the protein-peptide complex), or neutral (a hit both in the *apo* and the 14-3-3σ/ERα-pp complex; Figure 1c). C38 yielded the highest fraction of cooperative hits, but the maximal percent tethering was low (<55% conjugated), suggesting that fragments bound to C38 had a low affinity for the pocket. Conversely, C45, closest to the target pocket, yielded a large fraction of hits with >75% conjugation, with more competitive than cooperative hits. Satisfyingly, C42, with an intermediate position, yielded hits for both *apo* and ERα-pp bound 14-3-3σ, suggesting an optimal distance and orientation towards the target pocket to identify potent and cooperative fragments.

For C42, the most cooperative fragment was **1**; tethering increased 2.3-fold, from 26% (*apo*) to 60% (protein-peptide complex) (Figure 2a). A nearly identical compound, **2**, was identified in both screens, with 46% tethering to the *apo* 14-3-3σ and 59% tethering to the complex (Figure 2b). Compounds **1, 2,** and seven additional fragments that bound to the 14-3-3σ(C42)/ERα-pp complex were selected for follow-up experiments (see Figure S1 for mass spectra).

The 14-3-3σ(C42)-binding hits were confirmed in dose-response experiments detected by intact protein MS. Both **1** and **2** demonstrated strong preferential binding to the 14-3-3σ/ERα-pp complex over the 14-3-3σ protein alone (Figure 2c). Binding of the tethered fragment **2** was improved ~300-fold, from an effective concentration (EC_{50}) ~1 mM for *apo* to EC_{50} = 3 μM for the ERα-pp bound 14-3-3σ. Fragment **1**, the N-methylated version of **2**, showed an EC_{50} ~100 μM for binding to *apo* but remained >80% tethered to 14-3-3σ bound to ERα-pp down to 100 nM fragment, even in the stringent disulfide-reducing condition of 1 mM βME. Cooperative binding was less pronounced for the other primary screening hits (data not shown).

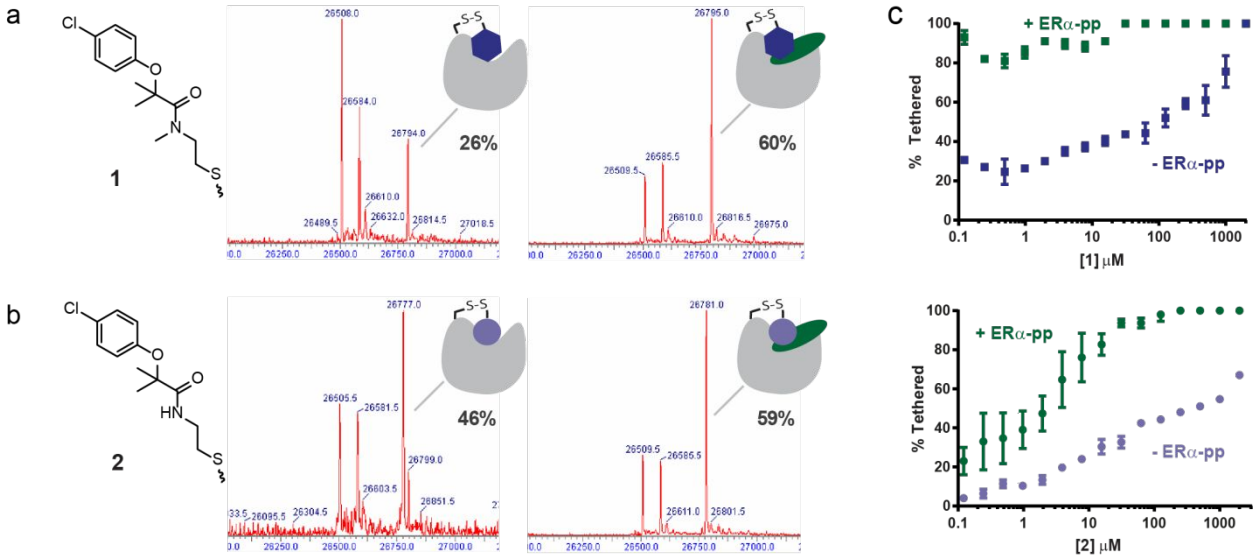

Figure 2. a) LC/MS spectra of tethering screen results for **1** conjugated to 14-3-3σ(C42) *apo* (left) or ERα-pp bound (right), resulting in 26% and 60% tethering, respectively. 14-3-3σ(C42) expected mass: 26509 Da, βME capped mass: 26585 Da, protein-disulfide conjugate mass: 26795 Da. b) LC/MS spectra of tethering screen results for **2** conjugated to 14-3-3σ(C42) *apo* (46%) or ERα-pp bound (59%); protein-disulfide conjugate mass: 26781 Da. c) LC/MS dose-response curves for **1** (top) and **2** (bottom) showing percentage of fragment-protein conjugate formation for titrations of disulfides to 14-3-3σ(C42) *apo* (■/●) and bound to ERα-pp (■).

The effect of **1** and **2** on the binding affinity between ERα-pp and 14-3-3σ(C42) was studied in fluorescence anisotropy experiments. 14-3-3σ(C42) was titrated into fluorescein-labeled ERα-pp in the presence of DMSO or saturating concentrations of fragments (Figure 3a). The apparent dissociation constant of 14-3-3σ(C42)/ERα-pp ($K_{d,app}$) was 1.3 μM for the DMSO control, and decreased to 32 nM in the presence of **1**, 92 nM in the presence of fragment **2**, and 4.2 nM in the presence of the positive control FC-A. Thus, **1** and **2** stabilized the 14-3-3σ/ERα-pp complex by 40- and 14-fold, respectively.

We observed the same trend when we titrated the fragments into a mixture of 1 μM 14-3-3σ(C42) and 100 nM fluorescein-ERα-pp, conditions under which half of the peptide was initially bound (Figure 3b). Fragments binding to the 14-3-3σ(C42)/ERα-pp complex increased the anisotropy, and hence the bound fraction, of fluorescein-ERα-pp. Additionally, from these experiments we observed that the kinetics of disulfide formation (i.e. stabilizing effect on ERα-pp binding) was dependent on the disulfide-fragment concentration, as evidenced by an increase in anisotropy values over time for 0.1-10 μM (Figure S2). The maximum effect was instantaneous at a saturating concentration (100 μM). Compound **1** displayed slightly more cooperative behavior, as reflected in a lower EC_{50} (87 nM) compared to **2** (EC_{50} = 209 nM). Notably, both were slightly more potent compared to FC-A (EC_{50} = 216 nM).

Whereas this cooperative behavior for **1** was expected based on the initial criteria for hit selection, **2** was only slightly

cooperative in the primary screen. To evaluate whether the single-concentration screen was reproducible, we further evaluated ten additional fragment hits, including three selected as 'competitive' from the screen (Figures S1, S3). While moderate cooperativity was observed for most of the 'cooperative' fragments, the competitive and neutral fragments generally had no effect on ERα-pp binding, except for one 'neutral' fragment that modestly inhibited peptide binding. Thus, while single-concentration screening yielded reproducible cooperative fragments, screening at multiple doses could be advantageous.

To elucidate the molecular mechanism for cooperativity, fragments were soaked into co-crystals of 14-3-3σ an 8-mer ERα-pp. In addition to **1** and **2**, electron density was resolved for three other C42 hits (see Table S1 for XRD statistics). Fragments **1-5** each contained an aromatic ring pointed into the back of the 14-3-3 pocket, oriented to make hydrophobic contact with the C-terminal V595 of ERα-pp (Figure 3c+d). The chlorophenyl substitutions in **1**, **2**, and **3** were fully buried in the pocket. Whereas for **1**, **2**, and **4** continuous electron density could be traced from the bound cysteine, **3** and **5** had less complete density, perhaps suggesting disorder in their linker region. Interestingly, while all fragments had a phenyl ring in an analogous location, **3-5** showed significantly less cooperativity compared to **1** and **2** (Figure S3a). These data could suggest that the electronic nature of the ring and/or the stability of the ring orientation are critical for productive interactions with both 14-3-3σ and ERα-pp.

Comparison of hits from screening C42 and C45 revealed **6**, which differed from **2** only in linker length (propyl vs ethyl, respectively) between the fragment and the disulfide-forming thiol. We solved the structure of **6** conjugated to 14-3-3σ(C45) in complex with ERα-pp and found electron density for the expected tethered fragment and parts of the linker (Figure 3e). An overlay of **6**-C45 with **2**-C42 showed that the chloride moiety was positioned in the same pocket of 14-3-3, but the chlorophenyl ring was tilted so that the edge, rather than the face, of the phenyl ring was pointed towards ERα-pp V595. Indeed, **6** displayed low cooperativity when bound to 14-3-3σ(C45) (Figure S4). Interestingly, **6** bound to 14-3-3σ(C42) showed similar cooperativity and binding affinity compared to **2** (EC_{50} value of < 1 μM in the presence of ERα-pp; Figure S4). The convergent positioning of the C42- and C45-targeted analogs **2** and **6** suggested that the fragments were selected based on their compatibility with the pocket formed by 14-3-3 and ERα-pp; however, the conformational restriction imposed by the anchoring residue determined how productively the fragment interacted with ERα-pp.

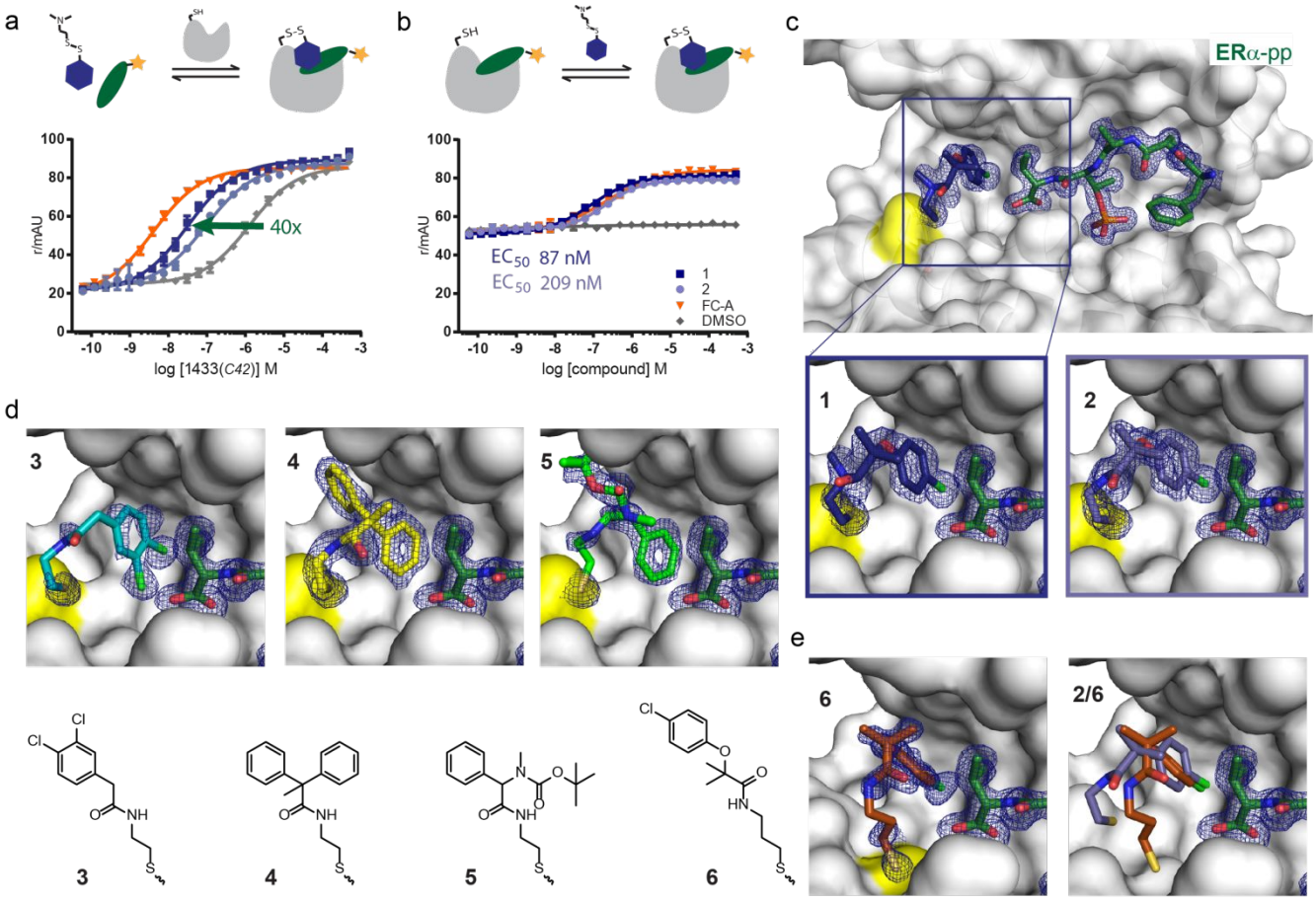

Figure 3. Quantification and mechanism of 14-3-3σ/ERα-pp stabilization. a) Schematic of experimental design and plot of anisotropy (mean + SD) for 14-3-3σ(C42) titrations to fluorescein-ERα-pp and saturating (100 μM) **1** (■), **2** (●), FC-A (▼) or DMSO control (◆), reporting a 40-fold increase of the 14-3-3σ(C42)/ERα-pp binding affinity in the presence of **1** (green arrow). b) Schematic of experimental design and plot of anisotropy (mean + SD) for titrations of **1** (■), **2** (●), FC-A (▼) or DMSO (◆) to fluorescein-ERα-pp and 1 μM 14-3-3σ(C42). c+d) X-

ray crystal structures of fragments **1** - **5** (colored sticks) in complex with 14-3-3σ(C42) (white surface; C42 yellow) and ERα-pp (green sticks). e) Fragment **6** conjugated to C45 and overlay with **2** bound to C42. All 2Fo-Fc electron density maps contoured at 1σ.

Together, the data for disulfide hits **1**, **2** and **6** supported the hypothesis that the binding affinity of the fragments to the protein-peptide complex was driven by non-covalent interactions, which was further enhanced by the linker. To confirm, we tested a non-covalent analogue for binding to 14-3-3/ERα-pp by ligand-observed NMR in $T_1\rho$ and waterLOGSY experiments (Figure S5). $T_1\rho$ relaxation was significantly enhanced in the presence of 14-3-3/ERα-pp (Figure S5a) and a positive wateLOGSY signal was seen in the presence, but not in the absence, of 14-3-3/ERα-pp (Figure S5b). These data demonstrated that the fragment bound to the complex even in the absence of a covalent linkage.

Finally, to investigate the selectivity of disulfide fragments for 14-3-3/ERα-pp, we selected the binding motifs of ExoS and TAZ as representative alternative 14-3-3 clients (Figure 4a).[29,30] The TAZ phosphopeptide (TAZ-pp) extends through the druggable pocket, thereby restricting the space for fragment binding. ExoS is one of the few reported non-phosphorylated clients of 14-3-3, and also occupies almost the full length of the amphipathic groove, including the target pocket. We also included TASK3, which contains a C-terminal phosphoSV nearly identical to the phosphoTV motif in ERα.[31] In dose-response analysis by MS, a shift to the left was observed for the binding curve of **2** in the presence of TASK3 phosphopeptide (TASK3-pp) compared to *apo* 14-3-3σ(C42), indicating a similar ability for **2** to bind cooperatively to the 14-3-3σ(C42)/TASK3-pp and ERα-pp complexes, with EC_{50} values of 7 μM and 3 μM, respectively. By contrast, for ExoS or TAZ-pp, the dose-response curve for binding of **2** was shifted to the right. Even at 500 μM, **2** just reached ~40% bound, compared to 80% bound to *apo* 14-3-3σ(C42), and 100% bound to 14-3-3σ(C42)/ERα-pp or TASK3-pp (Figure 4b). The effect of **2** on the binding affinity of 14-3-3σ(C42) for the different peptide partners was further quantified by fluorescence anisotropy, where **2** was titrated into a solution of fluorescently labeled TASK3-pp, ExoS, or TAZ-pp and 14-3-3σ(C42) at a concentration that allowed 20% binding of the peptide initially (Anisotropy (r) of ~40 mAU; see Figure S6 for 14-3-3 binding curves). FC-A and DMSO were included as controls. In alignment with MS data, **2** increased the affinity between 14-3-3 and TASK3-pp (EC_{50} = 2 μM) and showed a destabilizing effect on ExoS and TAZ-pp binding (IC_{50} = 1.4 μM and 2μM, respectively) (Figure 4c). Interestingly, the maximal anisotropy value for TASK3-pp was lower when **2** was titrated compared to FC-A; this difference was not observed when **2** and FC-A were titrated to ERα-pp (Figure 3b). It might indicate a reduced stabilization of the distal regions of TASK3-pp. Furthermore, there was a 10-20 fold shift in the EC_{50} for the stabilizing vs inhibiting effect of **2** on the binding of ERα-pp (100-200 nM) compared to TASK3-pp, ExoS and TAZ-pp (1-2 μM), indicating already partial selectivity for the hit fragment that can be further exploited by chemical optimization.

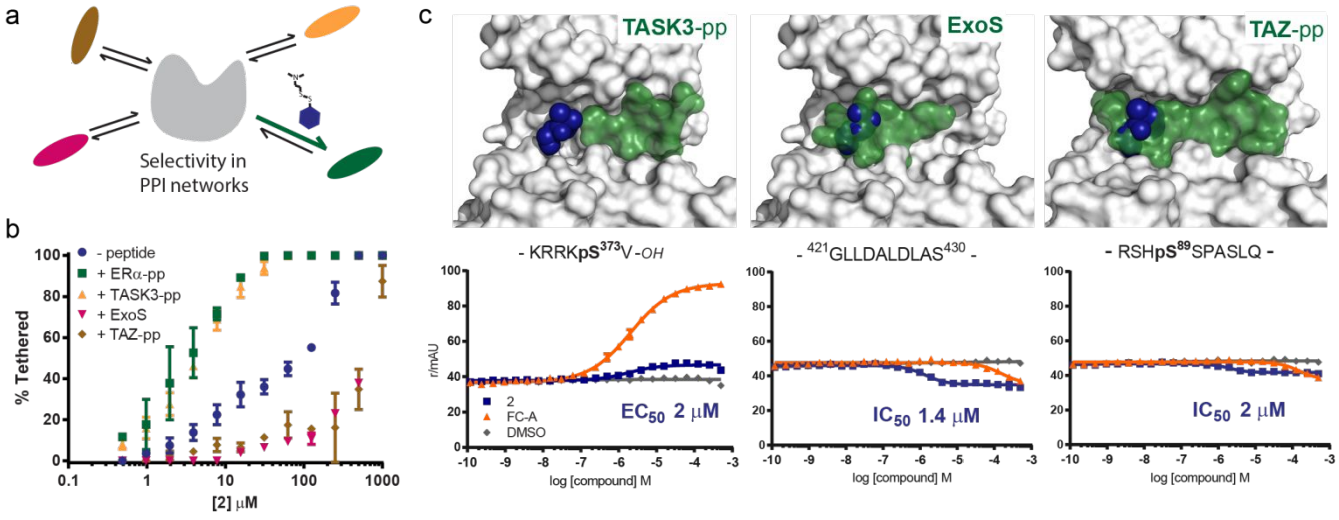

Figure 4. Selectivity of hit fragment **2**. a) Schematic illustration of the challenge posed by achieving selectivity in PPI network modulation. b) Dose-response curves obtained by MS, analyzing % tethering for titrations of **2** to 14-3-3σ *apo* (- peptide; ●) or bound to different interaction partner-derived peptide motifs; ERα-pp (■), TASK3-pp (▲), ExoS (▼) or TAZ-pp (◆), starting from 1 mM. c) Overlays of crystal structures of 14-3-3σ (white surface) bound by **2** (Figure 3c), and TASK3-pp (PDB: 3P1N), ExoS (PDB: 2O02) or TAZ-pp (PDB: 5N75) illustrating (in)compatibility of binding surface areas. Fragment (blue) and peptides (green) in space-filling representation. Fluorescence anisotropy data (mean + SD; triplicates) and non-linear fit for titration of **2** (■) to 14-3-3σ. FC-A (▼) and DMSO (◆) are included as controls.

Conclusions

Small-molecule PPI stabilization has diverse therapeutic applications, justifying the pursuit of novel drug discovery strategies. The major and unmet challenge in this field is the lack of starting points for small-molecule stabilizer development. In contrast to conventional screening techniques,

we find disulfide trapping to be highly suitable for early stabilizer discovery, likely because the technology is site-directed and the disulfide bond allows the fragment to fully saturate the binding site. We have validated the disulfide screening paradigm by selecting fragments that enhance the interaction between 14-3-3σ and an ERα-derived phosphopeptide (ERα-pp) and crystallized these fragments to learn the molecular requirements to achieve stabilization.

Disulfide-bound fragments bind cooperatively with ERα-pp to 14-3-3σ(C42), providing as much as a 40-fold increase in affinity for the 14-3-3σ(C42)/ERα-pp complex. Both the binding affinity and the degree of PPI stabilization depend on the chemical structure of the fragments and their orientation in the binding site. In particular, stabilization of the 14-3-3/ERα-pp complex correlated with the presence of para-chlorophenol ring oriented with its face towards the terminal valine of the peptide. Taken together, the biochemical data and crystal structures support the hypothesis that binding of the fragments was driven by the non-covalent interactions with the protein-peptide complex, which was confirmed in ligand-observed NMR experiments for a non-covalent analogue.

Towards development of the platform, we compared differential hits from three cysteine constructs of 14-3-3 and observed that the appropriate stringency of screening is essential for selecting fragments can engage the targeted pocket. In addition to the differences in the degree of tethering, we also observed that different types of hits (i.e. cooperative, neutral, competitive towards peptide binding) were more likely at different positions. Whereas we initially were very stringent towards selecting cooperative hits for follow-up, we found that 'neutral' hits displaying high intrinsic affinity for protein could also induce a cooperative effect when studied in more detail. Hence, future efforts could include multiple-dose screening to maximize the window between binding to 14-3-3 and to 14-3-3/peptide complexes.

One challenge when targeting PPI of proteins with many binding partners, such as 14-3-3, is client selectivity. Opportunities for selectivity result from the significant variation in phosphoprotein sequences and 14-3-3-binding modes, giving rise to differences in the protein-protein interface that small molecules could exploit. As demonstration, **2** shows the strongest cooperativity towards ERα-pp, secondly towards the ERα-like-peptide TASK3-pp, and at higher concentrations also partially influences the structurally unrelated 14-3-3/TAZ-pp or ExoS protein-peptide complexes. These differences could be further exploited by optimizing contacts with ERα-pp and tuning the ratio of intrinsic binding of the fragments to *apo*-14-3-3 versus binding to the 14-3-3/peptide complex.

It is important to note that 14-3-3 client proteins are much larger than the peptides studied here. However, 14-3-3 proteins exert their regulatory role specifically via phosphorylation-induced PPIs, and the phosphate group on a binding partner is usually the primary driver of the binding affinity. Therefore, even in the context of differential secondary interactions, a stabilizing effect on this primary interaction site will result in an overall increased stability of the full-length protein complex. To fully validate the utility of our fragments will require chemical optimization and characterization of the PPI in a biological environment. The principle innovation of these studies is the systematic platform for discovery of PPI stabilizing fragments that are then suitable for tried-and-true strategies to optimize fragments into chemical probes and/or drug leads.

The disulfide trapping strategy can be generalized to any 14-3-3/client pair. In addition to ERα, several other important transcription factors, including TAZ, Myc, RelA, and FOXO-1, are clients of 14-3-3, and this approach could conceivably develop modulators of multiple transcription factors. Furthermore, small molecules might be able to induce unnatural 14-3-3/protein complexes, allowing the exploration of synthetic biology. As a site-directed binding methodology, disulfide trapping is an ideal technology for such a platform approach. Systematic discovery of novel PPI stabilizers has the potential to access 'undruggable' targets and provide opportunities for intervention in previously inaccessible pathways.

Experimental Section

Protein expression and purification. The 14-3-3 σ isoform with a truncated C-terminus after T231 (ΔC; to enhance crystallization) and an N-terminal His_6-tag was expressed in NiCo21 (DE3) competent *E.coli* (New England biolabs Inc) from a pPROEX HTb expression vector. Site-directed mutagenesis to obtain double mutants C38N/N42C and C38N/S45C was performed using the QuickChange Lightening site-directed mutagenesis kit (Agilent Technologies) following manufacturer's instructions. C38N was selected since asparagine is the most prevalent amino acid at that position across the 14-3-3 family. Primer sequences are listed in SI Table S2. Constructs were confirmed by DNA sequencing. After transformation following manufacturer's instructions, single colonies were picked to inoculate 30 mL pre-cultures (LB), which were added to 1.5 L 2XYT medium after overnight growth at 37°C, 250 rpm. Expression was induced upon reaching OD_{600} 0.5-0.6 by adding 400 μM IPTG. After overnight expression at 18°C, 140 rpm, cells were harvested by centrifugation at 8000 rpm and resuspended in lysis buffer (50 mM Tris, pH 8.0, 300 mM NaCl, 10 mM imidazole, 5 mM $MgCl_2$, 1 mM PMSF, 250 μM TCEP). The His_6-tagged proteins were first purified by Ni-affinity chromatography (HisTrap HP column, GE) (Elution buffer 50 mM Tris, pH 8.0, 300 mM NaCl, 250 mM imidazole, 250 μM TCEP), followed by His-tag cleavage by TEV protease during dialysis (25 mM HEPES pH 7.5, 200 mM NaCl, 5% glycerol, 10 mM $MgCl_2$, 250 μM TCEP) overnight at 4°C. The flow-through of a second HisTrap column was subjected to final purification step by size-exclusion chromatography (Superdex75, GE) (SEC buffer 25 mM HEPES pH 7.5, 100 mM NaCl, 10 mM $MgCl_2$, 250 μM TCEP). The protein was concentrated to ~60 mg/mL, analyzed for purity by SDS-PAGE and Q-Tof LC/MS and aliquots flash-frozen for storage at -80°C.

Peptide sequences. Peptides for disulfide trapping were purchased from Elim Biopharmaceuticals, Inc. (Hayward, CA) Sequences were as follows: *Ac*-KYYITGEAEGFPA{pT}V-*COOH* (ERα-pp); *Ac*-RRK{pS}V-*COOH* (TASK3-pp); *Ac*-RSH{pS}SPASLQLGT-$CONH_2$ (TAZ-pp); *Ac*-SGHGQGLLDALDLAS-$CONH_2$ (ExoS). ERα-pp for X-ray crystallography and fluorescein-labeled peptides were ordered from GenScript Biotech Corp. Sequences were: *Ac*- or *5-FAM*-AEGFPA{pT}V-*COOH* (8mer ERα-pp) and *5-FAM*-labeled sequences as above for TASK3-pp, TAZ-pp and ExoS.

Disulfide Tethering screening and data processing. The primary screening was performed by incubating the target with individual compounds in a 384-well plate format. A custom

library of 1600 disulfide-containing fragments of the UCSF Small Molecule Discovery Center (SMDC), synthesized as previously reported, was available as 50 mM stock solutions in DMSO.[32,33] For screening, 14-3-3σ wild-type and Cys-mutants were diluted to 100 nM in buffer (10 mM Tris, 100 μM betamercaptoethanol (βME), pH 8.0) and plated in 384-well plates (15 μL/well). 30 nL of each fragment was pinned from the library master plates into the protein samples using a Biomek FX (Beckman) to give a final concentration of 100 μM. The duplicate experiments additionally contained 200 nM ERα-pp. The reaction mixtures were incubated for 3 hours at RT before being subjected to LC/MS (I-class Acquity UPLC / Xevo G2-XS Quadrupole Time of Flight mass spectrometer, Waters). Data collection and automated processing followed a custom workflow, as previously described.[28] All compounds described in the text were from the same lot as the original screening material.

Dose-Response LC/MS experiments. Disulfide tethering dose-response analysis used the same procedures as primary screening, with the exception that the βME concentration was 1 mM, and compounds were titrated from 5-50 mM in 2-fold serial dilutions in DMSO, then 400 nL of the compound was transferred to 10 μL protein solution for final concentrations 0.1-2000 μM and 4% DMSO. For the dose-response of **2** in the presence of TAZ-pp (150 μM), a 5 minute chromatography step was employed to separate the hydrophobic peptide from the 14-3-3 before ionization.

Fluorescence Anisotropy. Fluorescein-labeled peptides, 14-3-3 protein, FC-A (10 mM stock solution in DMSO) and disulfide fragments (50 mM stock solutions in DMSO) were diluted in buffer (10 mM HEPES pH 7.5, 150 mM NaCl, 0.1% TWEEN-20, 1 mg/mL Bovine Serum Albumine (BSA; Sigma Aldrich)). Final DMSO concentration in the assay was always 1%. Dilution series of 14-3-3 protein or fragments were made in black, round-bottom 384-microwell plates (Corning) in a final sample volume of 10 μL in triplicates. Fluorescence anisotropy measurements were performed directly and after overnight incubation at room-temperature, using a Tecan Infinite F500 plate reader (filter set λ_{ex}: 485±20 nm, λ_{em}: 535±25 nm). Data reported are at endpoint. EC_{50} values were obtained from fitting the data with a four-parameter logistic model (4PL) in GraphPad Prism 6.

X-Ray Crystallography. 14-3-3 protein (470 μM; 12.5 mg/mL) was mixed with ERα-pp (1:2 molar stochiometry; 940 μM) and incubated in buffer (20 mM HEPES pH 7.4, 2 mM $MgCl_2$, 2 mM βME overnight at 4°C before setting up for sitting drop crystallization in MRC crystallization plates (Swissci) with a custom crystallization liquor-grid (0.095 M HEPES (pH 7.1, 7.3, 7.5, 7.7), 0.19 M $CaCl_2$, 5% glycerol, 24-29% PEG 400). Crystals grew at 4°C within 4 days. Soaking of crystals was performed by mixing 0.4 μL disulfide fragments from 50 mM stock solutions in DMSO with 2 mM βME in 3.6 μL mother liquor, and adding this to crystal-containing drops. Soaked crystals were fished after overnight incubation and flash-frozen in liquid nitrogen. Data collection and processing are described in Supporting Information.

ASSOCIATED CONTENT

Supporting Information

The Supporting Information is available free of charge on the ACS Publications website.

XRD experimental details, data collection and refinement statistics; synthetic procedure; NMR spectroscopy methods; primer sequences for mutagenesis; deconvoluted MS screening data; anisotropy titration curves for **1** – **5** and seven additional screening hits; dose-response data (MS and anisotropy) for **6**; ligand-observed NMR spectra; and 14-3-3 titration curves to various binding partners. (Tables S1-S2 and Figures S1-S6) (PDF)

AUTHOR INFORMATION

Corresponding Authors

*c.ottmann@tue.nl
*michelle.arkin@ucsf.edu

Author Contributions

⊥These authors contributed equally to this work.

Notes

The authors declare no competing financial interests.

ACKNOWLEDGMENTS

We thank the Renslo laboratory for synthesis of the SMDC disulfide library, Connie Merron and Julia Davies for automated MS data processing infrastructure at the SMDC, Jim Wells and Adam Renslo for helpful discussions. Joris Adriaans and Dongju Wang are thanked for synthesis and technical support. Bert de Boer is kindly acknowledged for his contributions in the initial stage of the 14-3-3/ERα project.
The research described was funded by the National Institutes of Health (R01AG044515); the Initial Training Network TASPPI (H2020 Marie Curie Actions of the European Commission, Grant Agreement 675179); and the Netherlands Organization for Scientific Research (NWO) (Gravity Program 024.001.035 and Vici grant 016.150.366). E.S. acknowledges the Nora Baart Foundation (NVBMB; KNCV) and the Hendrik Muller program.

REFERENCES

1. Berg, T. Modulation of protein-protein interactions with small organic molecules. *Angew. Chem. Int. Ed Engl.* **42**, 2462–81 (2003).
2. Wells, J. A. & McClendon, C. L. Reaching for high-hanging fruit in drug discovery at protein-protein interfaces. *Nature* **450**, 1001–9 (2007).
3. Arkin, M. R., Tang, Y. & Wells, J. A. Small-Molecule Inhibitors of Protein-Protein Interactions: Progressing toward the Reality. *Chem. Biol.* **21**, 1102–1114 (2014).
4. Scott, D. E., Bayly, A. R., Abell, C. & Skidmore, J. Small molecules, big targets: drug discovery faces the protein-protein interaction challenge. *Nat. Rev. Drug Discov.* **15**, 533–550 (2016).
5. Fischer, G., Rossmann, M. & Hyvönen, M. Alternative modulation of protein-protein interactions by small molecules. *Curr. Opin. Biotechnol.* **35**, 78–85 (2015).
6. Andrei, S. A., Sijbesma, E., Hann, M., Davis, J., O'Mahony, G., Perry, M. W. D., Karawajczyk, A., Eickhoff. J., Brunsveld, L., Doveston, R. G., Milroy, L.-G. & Ottmann, C. Stabilization of protein-protein interactions in drug discovery. *Expert Opin. Drug Discov.* **12**, 925–940 (2017).
7. Zarzycka, B., Kuenemann, M. A., Miteva, M. A., Nicolaes, G. A. F., Vriend, G. & Sperandio, O. Stabilization of protein–protein interaction complexes through small molecules. *Drug Discov. Today* **21**, 48–57 (2016).

8. Waring, M. J., Chen. H., Rabow, A. A., Walker, G., Bobby, R., Boiko, S., Bradbury, R. H., Callis, R., Clark, E., Dale, I., Daniels, D. L., Dulak, A., Flavell, L., Holdgate, G., Jowitt, T. A., Kikhney, A., McAlister, M., Méndez, J., Ogg, D., Patel, J., Petteruti, P., Robb, G. R., Robers, M. B., Saif, S., Stratton, N., Svergun, D. I., Wang, W., Whittaker, D., Wilson, D. M. & Yao, Y. Potent and selective bivalent inhibitors of BET bromodomains. *Nat. Chem. Biol.* **12**, 1097–1104 (2016).
9. Bulawa, C. E., Connelly, S., Devit, M., Wang, L., Weigel, C., Fleming, J. A., Packman, J., Powers, E. T., Wiseman, R. L., Foss, T. R., Wilson, I. A., Kelly, J. W. & Labaudinière R. Tafamidis, a potent and selective transthyretin kinetic stabilizer that inhibits the amyloid cascade. *Proc. Natl. Acad. Sci. U. S. A.* **109**, 9629–9634 (2012).
10. Hughes, S. J. & Ciulli, A. Molecular recognition of ternary complexes: a new dimension in the structure-guided design of chemical degraders. *Essays Biochem.* **61**, 505–516 (2017).
11. Erlanson, D. A., Braisted, A. C., Raphael, D. R., Randal, M. Stroud, R. M., Gordon, E. M. & Wells, J. A. Site-directed ligand discovery. *Proc. Natl. Acad. Sci. U. S. A.* **97**, 9367–9372 (2000).
12. Ostrem, J. M., Peters, U., Sos, M. L., Wells, J. A. & Shokat, K. M. K-Ras(G12C) inhibitors allosterically control GTP affinity and effector interactions. *Nature* **503**, 548–51 (2013).
13. Erlanson, D. A., Arndt, J. W., Cancilla, M. T., Cao, K., Elling, R. A., English, N., Friedman, J., Hansen, S. K., Hession, C., Joseph, I., Kumaravel, G., Lee, W. C., Lind, K. E., McDowell, R. S., Miatkowski, K., Nguyen, C., Nguyen, T. B., Park, S., Pathan, N., Penny, D. M., Romanowski, M. J., Scott, D., Silvian, L., Simmons, R. L., Tangonan, B. T., Yang, W. & Sun, L. Discovery of a potent and highly selective PDK1 inhibitor via fragment-based drug discovery. *Bioorg. Med. Chem. Lett.* **21**, 3078–3083 (2011).
14. Hyde, J., Braisted, A. C., Randal, M. & Arkin, M. R. Discovery and characterization of cooperative ligand binding in the adaptive region of interleukin-2. *Biochemistry* **42**, 6475–6483 (2003).
15. Raimundo, B. C., Oslob, J. D., Braisted, A. C., Hyde, J., McDowell, R. S., Randal, M., Waal, N. D., Wilkinson, J., Yu, C. H. & Arkin, M. R. Integrating fragment assembly and biophysical methods in the chemical advancement of small-molecule antagonists of IL-2: an approach for inhibiting protein-protein interactions. *J. Med. Chem.* **47**, 3111–3130 (2004).
16. Molzan, M. & Ottmann, C. Synergistic Binding of the Phosphorylated S233- and S259-Binding Sites of C-RAF to One 14-3-3ζ Dimer. *J. Mol. Biol.* **423**, 486–495 (2012).
17. Sluchanko, N. N., Beelen, S., Kulikova, A. A., Weeks, S. D., Antson, A. A., Gusev, N. B. & Strelkov, S. V. Structural basis for the interaction of a human small heat shock protein with the 14-3-3 universal signaling regulator. *Struct. Lond. Engl. 1993* **25**, 305–316 (2017).
18. De Vries-van Leeuwen, I. J., Da Costa Pereira, D., Flach, K. D., Piersma, S. R., Haase, C., Bier, D., Yalcin, Z., Michalides, R., Feenstra, K. A., Jiménez, C. R., De Greef, T. F., Brunsveld, L., Ottmann, C., Zwart, W. & De Boer, A. H. Interaction of 14-3-3 proteins with the estrogen receptor alpha F domain provides a drug target interface. *Proc. Natl. Acad. Sci. U. S. A.* **110**, 8894–9 (2013).
19. Schumacher, B., Mondry, J., Thiel, P., Weyand, M. & Ottmann, C. Structure of the p53 C-terminus bound to 14-3-3: Implications for stabilization of the p53 tetramer. *FEBS Lett.* **584**, 1443–1448 (2010).
20. Zhao, J., Meyerkord, C. L., Du, Y., Khuri, F. R. & Fu, H. 14-3-3 proteins as potential therapeutic targets. *Semin. Cell Dev. Biol.* **22**, 705–712 (2011).
21. Aghazadeh, Y. & Papadopoulos, V. The role of the 14-3-3 protein family in health, disease, and drug development. *Drug Discov. Today* **21**, 278–287 (2016).
22. Stevers, L. M., Sijbesma, E., Botta, M., MacKintosh, C., Obsil, T., Landrieu, I., Cau, Y., Wilson, A. J., Karawajczyk, A., Eickhoff, J., Davis, J., Hann, M., O'Mahony, G., Doveston, R. G., Brunsveld, L. & Ottmann, C. Modulators of 14-3-3 Protein–Protein Interactions. *J. Med. Chem.* **61**, 3755–3778 (2018).
23. Erlanson, D. A., Wells, J. A. & Braisted, A. C. Tethering: fragment-based drug discovery. *Annu. Rev. Biophys. Biomol. Struct.* **33**, 199–223 (2004).
24. Pennington, K. L., Chan, T. Y., Torres, M. P. & Andersen, J. L. The dynamic and stress-adaptive signaling hub of 14-3-3: emerging mechanisms of regulation and context-dependent protein–protein interactions. *Oncogene* **37**, 5587 (2018).
25. Zhao, J., Du, Y., Horton, J. R., Upadhyay, A. K., Lou, B., Bai, Y., Zhang, X., Du, L., Li, M., Wang, B., Zhang, L., Barbieri, J. T., Khuri, F. R., Cheng, X. & Fu, H. Discovery and structural characterization of a small molecule 14-3-3 protein-protein interaction inhibitor. *Proc. Natl. Acad. Sci. U. S. A.* **108**, 16212–16216 (2011).
26. Milroy, L.-G., Bartel, M., Henen, M. A., Leysen, S., Adriaans, J. M., Brunsveld, L., Landrieu, I. & Ottmann, C. Stabilizer-Guided Inhibition of Protein–Protein Interactions. *Angew. Chem. Int. Ed.* **54**, 15720–15724 (2015).
27. Andrei, S. A., Meijer, F. A., Neves, J. F., Brunsveld, L., Landrieu, I., Ottmann, C. & L.-G. Milroy. Inhibition of 14-3-3/Tau by Hybrid Small-Molecule Peptides Operating via Two Different Binding Modes. *ACS Chem. Neurosci.* **9**, 2639–2654 (2018).
28. Hallenbeck, K. K., Davies, J. L., Merron, C., Ogden, P., Sijbesma, E., Ottmann, C., Renslo, A. R., Wilson, C. & Arkin, M. R. A Liquid Chromatography/Mass Spectrometry Method for Screening Disulfide Tethering Fragments. *SLAS Discov.* **23**, 183–192 (2018).
29. Ottmann, C., Yasmin, L., Weyand, M., Veesenmeyer, J. L., Diaz, M. H., Palmer, R. H., Francis, M. S., Hauser, A. R., Wittinghofer, A. & Hallberg, B. Phosphorylation-independent interaction between 14-3-3 and exoenzyme S: from structure to pathogenesis. *EMBO J.* **26**, 902–913 (2007).
30. Sijbesma, E., Skora, L., Leysen, S., Brunsveld, L., Koch, U., Nussbaumer, P., Jahnke, W. & Ottmann, C. Identification of Two Secondary Ligand Binding Sites in 14-3-3 Proteins Using Fragment Screening. *Biochemistry* **56**, 3972–3982 (2017).
31. Anders, C., Higuchi, Y., Koschinsky, K., Bartel, M., Schumacher, B., Thiel, P., Nitta, H., Preisig-Müller, R., Schlichthörl, G., Renigunta, V., Ohkanda, J., Daut, J., Kato, N. & Ottmann, C. A Semisynthetic Fusicoccane Stabilizes a Protein-Protein Interaction and Enhances the Expression of K+ Channels at the Cell Surface. *Chem. Biol.* **20**, 583–593 (2013).
32. Burlingame, M. A., Tom, C. T. M. B. & Renslo, A. R. Simple One-Pot Synthesis of Disulfide Fragments for Use in Disulfide-Exchange Screening. *ACS Comb. Sci.* **13**, 205–208 (2011).
33. Turner, D. M., Tom, C. T. M. B. & Renslo, A. R. Simple Plate-Based, Parallel Synthesis of Disulfide Fragments using the CuAAC Click Reaction. *ACS Comb. Sci.* **16**, 661–664 (2014).

Table of Contents graphic (TOC)